



Multi-model ensemble projections of soil moisture drought over North Africa and the Sahel region under 1.5, 2, and 3 °C global warming

Ahmed Elkouk^{1,2,3} · Zine El Abidine El Morjani¹ · Yadu Pokhrel³ · Abdelghani Chehbouni^{4,5} · Abdelfattah Sifeddine⁶ · Stephan Thober⁷ · Lhoussaine Bouchaou^{2,5}

Received: 5 February 2021 / Accepted: 10 August 2021 / Published online: 24 August 2021
© The Author(s), under exclusive licence to Springer Nature B.V. 2021

Abstract

The intensification of soil moisture drought events is an expected consequence of anthropogenic global warming. However, the implication of 1.5–3 °C global warming on these events remains unknown over North Africa and the Sahel region, where soil moisture plays a crucial role in food security that largely depends on rainfed agriculture. Here, using a multi-model ensemble from the Inter-Sectoral Impact Model Intercomparison Project phase 2b, we estimate the changes in the spatiotemporal characteristics of soil moisture drought events under increased global mean temperature. A 3 °C global warming results in multi-year (up to 19 years) mega-drought events over North Africa compared to a maximum drought duration of 12 years under the 1.5 °C Paris Agreement target. These events are projected to transform from historically severe droughts into exceptional droughts and extend over an area that is 32% larger under 3 °C compared to that under 1.5 °C. Global warming also leads to a high intensification of Sahelian drought extremes, in particular, their duration (from 24 to 82 months between 1.5 and 3 °C) over the western parts and their severity everywhere. Even though the results highlight substantial uncertainties arising from climate forcing and impact models, the projections indicate a tendency toward unprecedented exacerbation of soil moisture droughts that could pose serious threats to food security of North African and Sahelian societies in the absence of effective mitigation and adaptation.

Keywords Global warming · Soil moisture · Drought · North Africa · Sahel

✉ Ahmed Elkouk
ahmed.elkouk@edu.uiz.ac.ma

1 Introduction

Droughts affect human livelihoods and the ecosystems by adversely impacting water resource availability and agriculture, among other inter-connected systems (Mishra and Singh 2010). In developing countries with arid and semi-arid climates, where human livelihood depends largely on rainfed agriculture, extreme droughts result in devastating impacts. In the Sahel region, persistent droughts during the 1970s and 1980s destroyed crops, killed livestock, and resulted in over 100,000 human deaths due to malnutrition and starvation that consequently lead to migration, and sometimes conflicts (Grolle 2015; Kandji et al. 2006; Mach et al. 2019; Maharatna 2014; Masih et al. 2014; von Uexkull et al. 2016). In North Africa, numerous prolonged droughts including the 1994–1995 drought in Morocco, 1992–2002 drought in Algeria and Tunisia, and most recently the 2015–2016 drought in Tunisia and Morocco had widespread impacts on crop production, livestock farming, gross domestic product (GDP), and rural employment (Bazza et al. 2018).

In North Africa and the Sahel region, economic growth, food safety, and stability depend strongly on climate variability and change. For example, rainfed agriculture in North Africa and the Sahel region is of high importance for the rural population, which is mostly poor (IFAD 2010). In these regions, the population relies heavily on rainfed farming as a source of food and income, especially in the Sahel where more than 70% of the total population lives in rural areas (Vgen and Gumbrecht 2012). In North Africa, more than 90% of agricultural areas depend entirely on precipitation regimes (Bazza et al. 2018). Based on GDP and employment data, the importance of agriculture in North Africa is suggested to range from medium in Libya and Algeria, to high in Tunisia, and very high in Morocco (Schilling et al. 2012).

The dependency of agriculture systems on climate leads to high vulnerability across the economic and social sectors throughout North Africa and the Sahel region (Schilling et al. 2020). The potential increase in drought frequency and severity and the shift in aridity in terms of location and extent are undoubtedly two of the most important consequences of climate change in these regions (Dai 2013; Greve and Seneviratne 2015; Huang et al. 2016; IPCC 2012; Orłowsky and Seneviratne 2013; Wang 2005; Zhao and Dai 2015). North African and Sahelian societies are therefore likely to suffer from climate change due to their vulnerability and lack of adaptation capacities (Niang et al. 2014a). A fast demographic growth which leads to increased water and food demands, combined with the depletion of land and environmental resources, is expected to aggravate population vulnerability and exacerbate future drought impacts across the region (Godfray et al. 2010; Khan et al. 2014; Niang et al. 2014a).

Droughts are nonlinear in nature: the cascade of translation from precipitation deficit (meteorological drought) to soil moisture deficit (agriculture drought) and surface and subsurface water depletion (hydrological drought) is not always complete and the lag time during this translation depends on various factors (Konapala and Mishra 2017; WMO 2018). No single variable (precipitation, soil moisture, or runoff) can thus capture all drought impacts (Wanders et al. 2017). Yet, soil moisture is considered an integrative indicator for drought assessment since it reflects the balance between rainfall, evapotranspiration, runoff, and drainage (Keyantash and Dracup 2002). Soil moisture drought can directly impact crop development and yield (Xu et al. 2019) which pose great threats to livestock farming and food security in transitional environments.

A likely increase in dry spell length and frequency is projected for the upcoming decades in terms of precipitation, soil moisture, and evapotranspiration in the Mediterranean region (including North Africa) as a result of anthropogenic global warming (Greve et al. 2014;

Greve and Seneviratne 2015; Hoegh-Guldberg et al. 2018; IPCC 2012; Orłowsky and Seneviratne 2013; Polade et al. 2017; Sheffield and Wood 2008; Wartenburger et al. 2017; Zhao and Dai 2015). Although significant uncertainties are associated with precipitation projections across the Sahel (Biasutti 2013; Diedhiou et al. 2018; IPCC 2013; James and Washington 2013; James et al. 2015; Monerie et al. 2017; Park et al. 2015), western (central and eastern) Sahel is generally projected to experience drier (wetter) conditions as global warming intensifies.

The Paris Agreement on climate change focused on limiting global warming levels to below 2 °C and pursuing efforts to hold warming to 1.5 °C above the pre-industrial levels. However, the impacts of these global temperature thresholds on soil moisture drought have not yet been fully assessed at the sub-regional and local scales. Previous studies quantified the changes in drought characteristics based on multiple emission scenarios that cover a wide range of global temperature projections (e.g., Greve et al. 2014; Orłowsky and Seneviratne 2013; Prudhomme et al. 2014; Zhao and Dai 2015). Moreover, drought assessments are commonly performed at the pixel level and ignore the spatiotemporal evolution of drought characteristics (e.g., duration and area) (Diedhiou et al. 2018; Klutse et al. 2018; Lehner et al. 2017; Naumann et al. 2018; Wartenburger et al. 2017) which can have an impact on trends and variability of these extremes (Zhan et al. 2020).

To address these shortcomings, the goal of this study is therefore to quantify the impact of 1.5, 2, and 3 °C warming levels on the spatiotemporal characteristics (severity-area-duration) of soil moisture drought events, examine their causes and correspondence to changes in other drought indicators, and assess uncertainty under each warming level. To perform this assessment, we used the multi-model ensemble hydrological simulations from the Inter-Sectoral Impact Model Intercomparison Project phase 2b (ISI-MIP2b) designed to support the IPCC Special Report on the impact of 1.5 °C global warming (Frierler et al. 2017). The ensemble consists of monthly soil moisture simulations from 8 Impact Models (IMs) driven by down-scaled and bias-adjusted climate forcing from 4 Global Climate Models (GCMs) under 3 representative concentration pathways (RCPs; 2.6, 6.0, and 8.5). The IMs used in this study cover a diverse range of process parametrizations which is a fundamental requirement for a comprehensive assessment of soil moisture drought under different global warming levels (Samaniego et al. 2018).

The remainder of the paper is organized as follows. First, we present the study domain, dataset, and methods. We then present the changes in the characteristics of extreme soil moisture drought events under different global warming levels relative to the historical period and show how consistent these changes are across the ensemble members. Next, the implications of changes in drought events are presented in terms of the change in soil moisture availability and their correspondence to changes in other drought indicators across different levels of global warming. Finally, we quantify the contribution of IMs and GCMs to the uncertainties associated with changes in drought conditions across the study domain.

2 Method

2.1 Dataset and study domain

The study domain includes the region of North Africa and Sahel. Figures S1–S3 (in the Supplementary information, SI) present the large diversity in topography, rainfall, and land

cover within the study domain. North Africa is defined as the region between (27° N–37° N; 18° W–30° E). This region experiences a Mediterranean climate with a wet season during winter and dry conditions in the summer. North African climate shows drier and warmer conditions from the north (and high mountains in the western parts, where annual rainfall is greater than 600 mm) to the south (where annual rainfall less than 100 mm). These differences lead to very diverse landscapes and hydrometeorological regimes throughout North Africa. The Sahel is defined as the region between (10° N–20° N; 18° W–30° E). This area is a semi-arid transition zone located between two climate regimes: the Sahara Desert to the north and the tropical regime to the south. The Sahel experiences a long dry season for most of the year, with a short wet season during the West African monsoon (July–September). Rainfall varies sharply from less than 100 mm in the north to more than 800 mm in the south which dictates the progression of natural land cover. The Sahel region is also characterized by very diverse hydrometeorological regimes between its western, central, and eastern parts because of the difference in their locations in respect to the Atlantic and the planetary Hadley circulation. To enhance comparability with previous studies, we divided the Sahel domain into two sub-regions of western Sahel (10° N–20° N; 18° W–0°) and central-eastern Sahel [10° N–20° N; 0°–30° E]. Note that areas where annual mean precipitation is less than 100 mm are not included in the study domain (white color in Fig. S1). Soil moisture-based drought assessment in these hyper-arid areas is meaningless, since soils are rather dry most of the time.

A multi-model ensemble of monthly soil moisture is assembled from all available simulations of the ISI-MIP2b project (Frieler et al. 2017). The ensemble consists of soil moisture output from eight global IMs (Table S1) which include four land surface models (LSMs): CLM 4.5 (Thiery et al. 2017), JULES-W1 (Best et al. 2011), ORCHIDEE (Guimberteau et al. 2018), and MATSIRO (Pokhrel et al. 2015; Takata et al. 2003); three Global Hydrological Models (GHMs): H08 (Hanasaki et al. 2018), PCR-GLOBWB (Wada et al. 2014), and WaterGAP2 (Müller Schmied et al. 2016); and one dynamic vegetation model (DVM, regarded here as an LSM): LPJmL (Sitch et al. 2003). The IMs are driven by climate forcing data from four GCMs (GFDL-ESM2M, IPSL-CM5A-LR, HadGEM2-ES, and MIROC5). The GCMs were selected to cover the uncertainty range of precipitation and temperature in the phase 5 of the Coupled Model Intercomparison Project CMIP5 (Frieler et al. 2017). GCMs forcing data were first downscaled to a spatial resolution of 0.5° by 0.5° (~50 km at the equator) and bias-adjusted to observed data for both the historical simulations (1861–2005) and future climate projection (2006–2100) under three RCPs (RCP 2.6, 6.0, and 8.5).

In this study, the 30-year period 1971–2000 is selected to represent the historical (near present-day) climate conditions. Future conditions, on the other hand, are defined as the 30-year periods (Table S2) when global 30-year average temperature increases by three policy-relevant warming levels of 1.5, 2, and 3 °C relative to global warming during the historical period (estimated around 0.46 °C relative to the pre-industrial period 1881–1910). The future warming periods are defined following the time sampling approach reviewed in James et al. (2017). Further details are provided in Section S1 in Supplementary information.

The ensemble members used in this study have been employed previously for a wide range of climate impact (including hydrological and agriculture drought) studies (e.g., Dottori et al. 2018; Edward et al. 2018; Grillakis 2019; Lange et al. 2020; Schewe et al. 2019). Their skill for reproducing observed streamflow percentiles was analyzed globally in numerous works and found to reasonably reproduce observations over West African catchments (Veldkamp et al. 2018; Zaherpour et al. 2018). Moreover, the ensemble shows high skill in capturing terrestrial water storage (TWS) observation from the Gravity Recovery and Climate

Experiment, particularly in water-limited regimes (including the study domain) where TWS is mainly modulated by soil water content (Pokhrel et al. 2021; Pokhrel et al. 2012). Additionally, we compared the spatiotemporal characteristics of soil moisture drought events estimated from the multi-model ensemble against observations and reanalysis datasets during the historical period. Overall, the multi-model ensemble median shows a reasonably high skill in capturing drought characteristics, except for maximum drought duration which is only reproduced well by LSMs, likely due to relatively higher buffering capacity of deeper soil column in LSMs than in GHMs. More details on this evaluation exercise are provided in Section S4 in the Supplementary information.

Soil moisture content is simulated at different soil layers which depends on the different vertical discretization of the soil between IMs (Table S1). To approximate this variable across IMs, we integrated simulated soil moisture across soil layers to a depth of up to 1.5 m (depth differs between IMs, refer to Table S1 for the exact depths). We note that the simulated soil moisture state by IMs is largely a model-specific quantity (Fig. S4), “essentially an index of the moisture state” (Koster et al. 2009) rather than a physical quantity. These differences extend beyond those due to different soil layer depths (e.g., evaporation, interception, wilting point, hydraulic conductivity).

2.2 Identification of soil moisture drought events

Soil moisture content varies strongly across different IMs (Fig. S4). Thus, to ensure inter-comparability between IMs, monthly soil moisture is transformed into a quantile-based soil moisture index (*SMI*). Following Samaniego et al. (2013); (2018), the *SMI* is drawn from the cumulative distribution function of soil moisture timeseries estimated using a nonparametric kernel density estimate (KDE) to avoid making an assumption about the shape of the distribution which can introduce additional uncertainty in the drought analysis. The KDE is estimated for each calendar month, grid cell, and RCP/GCM/IM combination during the period 1861–2000. Using such a long period allowed us to robustly capture the form of the distribution function. The estimated KDE is then used as a reference to draw the *SMI* timeseries for the future periods corresponding to 1.5, 2, and 3 °C warming levels (refer to Section S2 in the Supplementary information for further details). The *SMI* represents monthly quantiles of soil moisture (Fig. S5) and thus varies between 0 (drier conditions) and 1 (wetter conditions).

Drought events are identified in space and time using a clustering algorithm previously developed and applied to study soil moisture drought in Germany and across Europe (Samaniego et al. 2013; Samaniego et al. 2018). In space, all cells where soil moisture is less than the value corresponding to the 20th percentile, i.e., $SMI \leq 0.2$, are consolidated into drought clusters. According to the US Drought Monitor classification (USDM; Svoboda et al. 2002), $SMI \leq 0.2$ reflects moderate drought conditions or even worse. To avoid cases where a drought event would shrink to small areas and persist for a long period of time (Sheffield et al. 2009; Wang et al. 2011), we excluded clusters with an area of less than 40 cells (~100,000 km²). Temporally, overlapping drought clusters at consecutive time steps are grouped into spatiotemporal drought events when their overlapping is greater than 20 cells (~50,000 km²). These large area thresholds are chosen due to the higher confidence in the ability of the multi-model ensemble to represent large-scale extremes than small-scale ones. It should be noted that using different area thresholds (20–60 cells) is found to have little effect on the rate of change of drought characteristics of the most extreme events between warming levels.

2.3 Calculation of drought statistics

A drought event can be characterized in terms of its duration, area (spatial extent), and severity. Duration is the time from the onset until the end of an event and equals the average number of months estimated over all the cells within a drought event. Area corresponds to the average region under drought from onset until the end of an event. Events duration and area are then combined with severity to draw the severity-area-duration (SAD) curves (Andreadis et al. 2005; Samaniego et al. 2013; Sheffield et al. 2009). Severity (S_d) is defined as the monthly *SMI* averaged over a duration d . Further details are provided in Section S3 in the Supplementary information. We choose to focus on changes in the most extreme events of the longest duration, maximum spatial extent, and highest severity. Such large-scale extremes often have the highest impacts on society and the environment and thus are of great relevance to stakeholders and water managers in drought-prone regions.

In order to assess the implications of future drought events, we estimate soil water content under drought conditions for different climate conditions (Samaniego et al. 2018). First soil moisture content corresponding to the 20th percentile is estimated independently for the historical and each warming period for each calendar month, each cell, and RCP/GCM/IM combination. Then, the change in available soil moisture content (Δx) is averaged over each season for all warming levels relative to the historical period (refer to Section S5 in the Supplementary information for further details). We also examine the causes of changes in soil moisture drought through their correspondence to other drought indicators represented by precipitation, atmospheric evaporative demand, evapotranspiration, and runoff.

2.4 Consistency and uncertainty assessment

The impact of global warming is quantified by calculating the change in drought conditions between the historical period (1971–2000) and 30-year periods corresponding to 1.5, 2, and 3 °C warming levels. To assess the consistency of this change, we quantify the percentage of ensemble members that agree on the direction of change in drought characteristics under each warming level. We then calculate the signal-to-noise ratio (SNR) to assess the uncertainty of the resulting projections. The SNR equals the median (signal) divided by the interquartile range (noise) of the multi-model ensemble projections. Finally, we assess the individual contribution of GCMs and IMs to the total uncertainty by applying Samaniego et al. (2017) sequential sampling approach (see Section S6 in the Supplementary information for further details).

3 Results

3.1 Changes in the spatiotemporal characteristics of extreme drought events under global warming

The analysis of the multi-model ensemble projections reveals high inter-model variability in the impact of global warming on the spatiotemporal characteristics of soil moisture drought across North Africa and Sahel (Fig. 1, S8, and S9). The duration of the longest events is projected to increase (>66% model agreement) under all global warming levels in North Africa (Fig. 1a). Median drought duration is projected to increase from 26 months during the

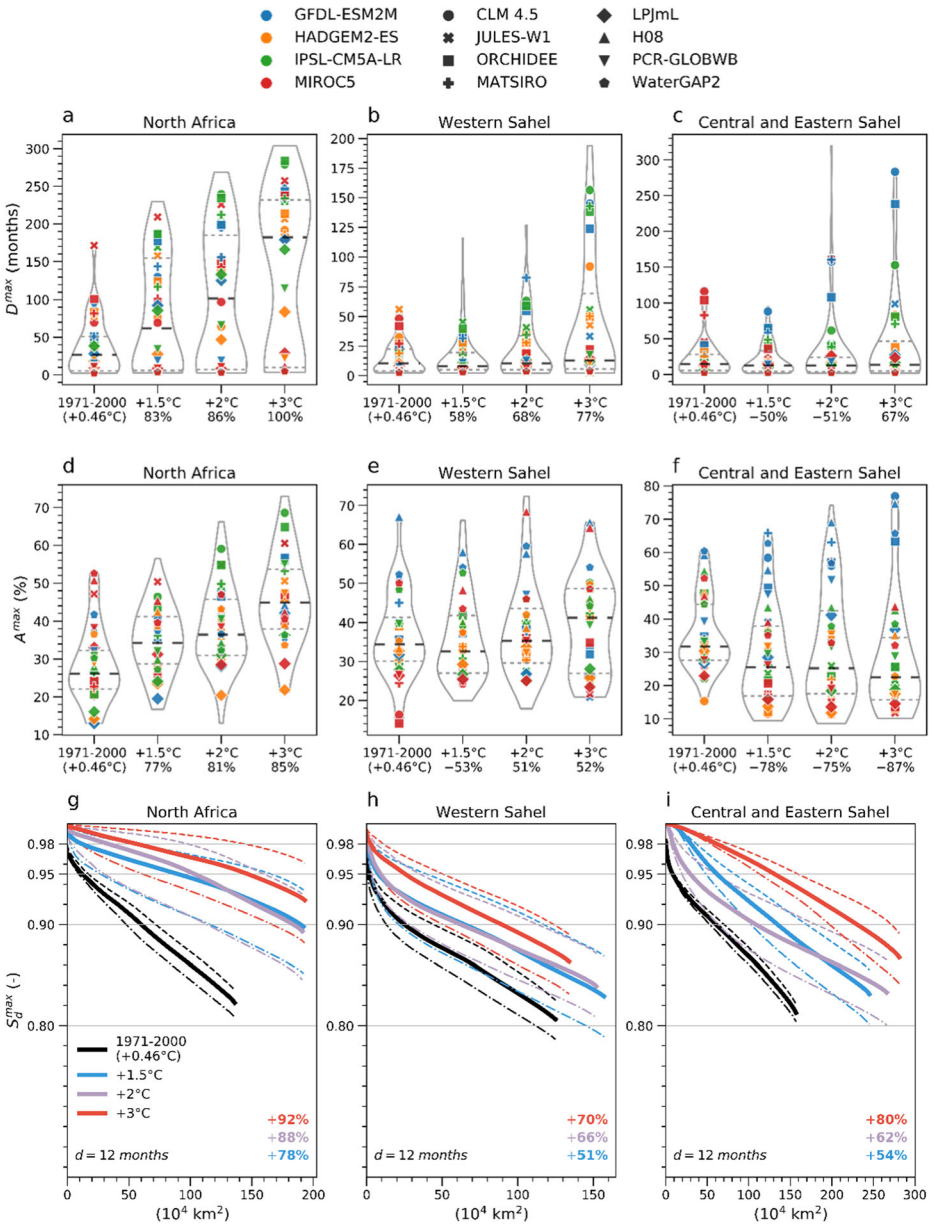
historical period to 61, 101, and 182 months (~5–15 years) under 1.5, 2, and 3 °C warming levels, respectively. This increase is associated with high inter-model variability, especially between GHMs and LSMs (Fig. 1a and S8). When only considering the LSM ensemble members (from which maximum drought duration in the historical period agrees well with observations), exceptional droughts are projected to last from 155 to 232 months (~12–19 years) between 1.5 and 3 °C global warming. This large exacerbation indicates that historical drought extremes will become normal conditions in the future, rather than extremes.

Although the ensemble median shows little change in maximum drought duration over the Sahelian domain, a robust increase (>66% model agreement) is projected under 3 °C warming (Fig. 1b, c). The magnitude of this increase varies depending on both GCMs and IMs (Fig. 1b and S8). Median duration estimates from three out of the four GCMs-driven LSMs show an increase from 24 to 82 months across Western Sahel between 1.5 and 3 °C warming levels. Over central and eastern Sahel, the increase is less substantial as drought extremes are projected to last from 38 to 50 months between 1.5 and 3 °C warming conditions.

Similar to drought duration, the area of the largest events is projected to increase (>66% model agreement) over North Africa with higher warming (Fig. 1d and S9). Median drought area is projected to increase from 34 to 45% between 1.5 and 3 °C warming conditions (that is an increase by 32% in relative terms). By contrast, global warming has little effect on the area of exceptional droughts in western Sahel (Fig. 1e). In its central and eastern parts, however, median drought area is projected to decrease (>66% model agreement) from 32 to 22% between the historical period and the 3 °C warming level (Fig. 1f and S9). Only the simulations driven by GFDL-ESM2M show an increase in drought area with higher global warming (Fig. 1f).

Drought duration and area are combined with drought severity (S_d) to obtain the SAD curves across the spatial scales of North Africa and Sahel. Figure 1g–i presents the ensemble projections of the SAD curves for the most severe drought events of 12-month duration. A robust increase (>66% model agreement) in event severity is projected across the spatial scales of North Africa under the three global warming levels (Fig. 1g). According to the USDM classification (Svoboda et al. 2002), historically severe drought events (S_d in [0.9, 0.95]) are projected to transform into exceptional events ($S_d \geq 0.98$) under 3 °C global warming. No substantial difference is found between the 3 °C and the 1.5 and 2 °C warming levels (Fig. 1g). A comparable increase (>66% model agreement) is also projected everywhere in the Sahel under 3 °C global warming (Fig. 1h, i). The intensification of drought severity is also found for both short-term (3-month) and long-term (24- and 48-month) droughts across the entire study domain (Fig. S10).

In summary, global warming results in a large and consistent (>66% model agreement) exacerbation of soil moisture drought events across North Africa. A 3 °C warming level could result in unprecedented drought conditions to a degree that historical extremes may be considered normal conditions in the future, which was also suggested for the Mediterranean region (Lehner et al. 2017; Naumann et al. 2018; Samaniego et al. 2018). Such conditions confirm the “dry gets drier” paradigm (Greve and Seneviratne 2015) across North Africa and indicate an alteration of the hydrologic regimes toward arid and hyper-arid conditions. The intensification of drought conditions can be substantially reduced, in particular event duration, with climate mitigation to keep warming below 1.5 °C. Ensemble projections throughout the Sahel, which are mostly consistent (>66% model agreement) under 3 °C global warming, suggest an intensification in drought events duration (especially over the western parts) and severity (across the whole region). These findings demonstrate that the exacerbation of soil moisture droughts is more intense and affects a much broader area than the intensification of meteorological droughts, which is found to be mostly confined to western Sahel (Diedhiou et al. 2018).



3.2 Implications and drivers of changes in drought events

We investigate the implications of future drought conditions in terms of the change in soil water content corresponding to the 20th percentile threshold (estimated independently for the

◀ **Fig. 1** Multi-model ensemble estimates of the spatiotemporal characteristics of exceptional drought events during the historical period (1971–2000, corresponding to 0.46 °C global warming) and 1.5, 2, and 3 °C global warming levels. Panels (a–c) present the average duration (in months) of the longest drought events (D^{max}). Panels (d–f) present the average area of the largest drought events (A^{max}), expressed as the percentage of the total area of each region. Panels (g–i) present the severity-area-duration curves for the most severe 12-month drought events (S_d^{max}). Violins in panels (a–f) display the distribution of the ensemble estimate of drought duration and area under the historical period and the three warming levels. Lines within each violin indicate the ensemble median (middle black dashed line) and interquartile range (75th–25th percentile for top and bottom gray dashed lines). Symbols within violins represent IMs/GCMs estimates averaged across the three RCPs. Lines in panels (g–i) indicate the ensemble median (solid lines) and interquartile range (dashed lines). Percentages (x-axis in panels a–f and lower-right corner in panels g–i) denote the level of model agreement on the direction change compared to the historical period. The y-axes in panels (g–i) are divided according to the USDM classification of abnormally dry (0.8–0.7), moderate drought (0.8–0.9), severe drought (0.9–0.95), extreme drought (0.95–0.98), and exceptional drought (0.98–1.0). For panels (a–f), the y-axis limits are different for clarity

historical period and global warming levels). The ensemble mean reveals a decrease in soil water availability (>66% model agreement) across North Africa under global warming (Fig. 2a, b). At a warming level of 3 °C, soil moisture content under drought conditions (Fig. 2a) is projected to decrease by 10%, especially during the winter season (December–February in Fig. S11a). This reduction is greater when considering mean soil moisture content (Figs. 2b and S11b), particularly across the northwestern (along the Mediterranean and Atlantic) much wetter parts of North Africa. The decrease in soil moisture availability, although small, leads to unprecedented exacerbation of exceptional drought events across North Africa, as was highlighted in the previous section. This result confirms previous assessments which showed that small changes in the long-term mean soil moisture lead to large increases in drought frequency (Zhao and Dai 2015).

A decline in soil water availability over North Africa is primarily related to a decrease in precipitation (Fig. 2c). Under 3 °C, winter precipitation (Fig. S11c) is projected to decrease by 28% (ranging from 19 to 47%) which is deemed very likely as a result of the suppression of subtropical rainfall due to the widening of the Hadley Circulation (IPCC 2013). The second key factor to soil water availability decline is the increase in atmospheric evaporative demand, reflected by the increase in potential evapotranspiration (Figs. 2g and S11g). This increase is mainly a result of a rising vapor pressure deficit due to increasing temperature and little changes in relative humidity (Scheff and Frierson 2014). Enhanced atmospheric demand for moisture is expected to aggravate drought conditions, even though it is not reflected in changes of actual evapotranspiration (Fig. 2d) which decreases due to the decline in precipitation supply. Drying is also projected for precipitation minus evapotranspiration (P-ET) and surface runoff (Fig. 2e, f), although less widespread compared to soil moisture drying.

For the large parts of the Sahel, the ensemble members show a low agreement on the direction of change in soil water availability under drought conditions (Fig. 2a). Nevertheless, changes in mean soil water availability (Fig. 2b) show a more consistent decrease (increase) over western (central and eastern) Sahel, in particular during the monsoon season (July–September in Fig. S12b). Changes in soil moisture reflect precipitation projections of a wetter Sahel everywhere but along the coastal western parts (Figs. 2c and S12c) which is consistent with both CMIP3 and CMIP5 ensemble mean projections (Biasutti 2013; Fontaine et al. 2011; James and Washington 2013; James et al. 2015; Monerie et al. 2017). The response of Sahel rainfall to global warming however is associated with high model disagreements on both the magnitude and the direction of trend (e.g., GFDL-ESM2M and MIROC5 in Fig. S13). Nevertheless, rainfall mean projections (Fig. S14) show a robust negative trend confined to

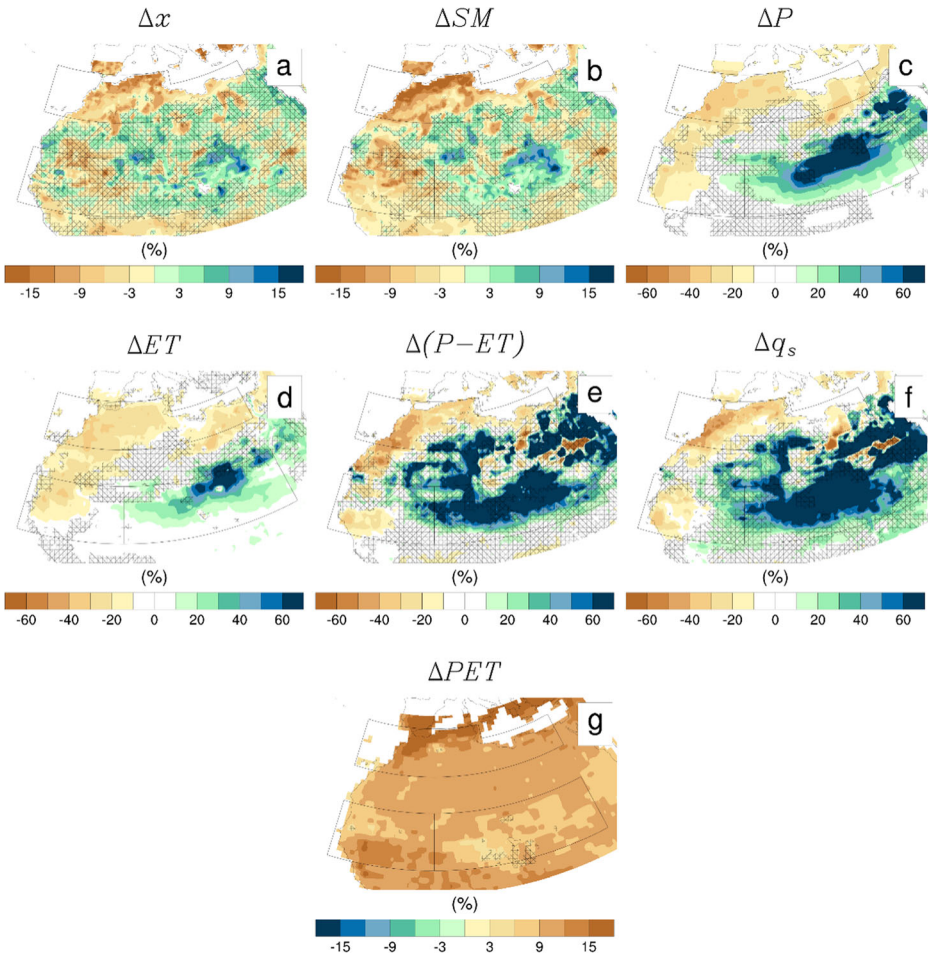


Fig. 2 Changes (global warming of 3 °C minus historical period) in water-year (October–September) (a) mean soil moisture under drought conditions (corresponding to the 20th percentile, Δx), (b) mean total soil moisture (ΔSM), (c) mean precipitation (ΔP), (d) mean evapotranspiration (ΔET), (e) mean precipitation minus evapotranspiration ($\Delta(P-ET)$), (f) mean surface runoff (Δq_s), and (g) mean Penman-Monteith potential evapotranspiration (ΔPET). Brown colors indicate drying, while blue indicates wetting (note the reverse of colors for ΔPET in panel g). Hatching indicates where <67% of the ensemble members agree on the sign of change of ensemble mean. Surface runoff projections were only available from six out of the eight IMs. Penman-Monteith PET is shown from one IM (i.e., ORCHIDEE)

western Sahel during the monsoon onset (June–July) and a robust positive trend that span the Sahel during the monsoon demise (September–October), in agreement with CMIP5 ensemble mean (Biasutti 2013). This behavior is suggestive of a delay of the West African Monsoon season in response to increasing greenhouse gases (Biasutti 2013; Biasutti and Sobel 2009; Mariotti et al. 2011; Seth et al. 2013; Sylla et al. 2015).

A wetter central and eastern Sahel is however in contrast to changes in drought characteristics (increasing duration and severity). First, this highlights that changes in the spatiotemporal characteristics of drought extremes, which are defined by the tail of the distribution, can vary greatly from changes in mean precipitation and soil moisture (Dai et al. 2018; Zhao and Dai

2015). Second, it suggests that an exacerbation of exceptional droughts in a wetter Sahel will be more driven by increasing atmospheric evaporative demand (Cook et al. 2018; Dai 2013) compared to drought events from the past (e.g., the 1970s–1980s) which mainly resulted from the reduction of summer rainfall (Dai 2013).

A change in the character of precipitation events was also found over the Sahel in terms of a decrease in their frequency but an increase in their intensity (Diallo et al. 2012; Diedhiou et al. 2018; Sylla et al. 2015). This change will likely lead to a wider drying as more water goes to surface runoff than to replenish the soil. This effect likely contributed to intensifying drought severity in central and eastern Sahel (e.g., 3-month duration in Fig. S10) as precipitation increase mostly runs off (Fig. 2f). The effects of the changing character of precipitation on drying in the Sahel, therefore, warrant further assessments.

The intensification of drought conditions across these transitional environments supports the hypothesis that the effects of elevated atmospheric CO₂ in the future, as simulated by LSMs (Table S1), would be negligible on vegetation water-use efficiency under drought conditions. This was suggested in several experimental studies and is due to stomatal closure in response to low soil water availability during a drought event (Tramblay et al. 2020). Under these conditions, soil moisture drought is expected to severely affect vegetation and biodiversity, threaten food security, and increase water abstraction across the region (Droogers et al. 2012; Niang et al. 2014b; Roudier et al. 2011; Sultan and Gaetani 2016). Therefore, the development of high-resolution multi-model projections of soil moisture will be of high relevance to water managers and practitioners (Samaniego et al. 2019). Adaptation assessments for agriculture systems in the region could substantially benefit from incorporating soil moisture because it is the primary source of water for crop development (Vergopolan et al. 2021).

3.3 Uncertainty assessment

To assess the uncertainty in drought projections, we computed the signal-to-noise ratio (SNR) as the ensemble median (signal) divided by the interquartile range (noise). Figure 3a presents the SNR calculated from the change in drought events characteristics, soil moisture, and hydrological drought indicators represented by P-ET and surface runoff. The SNR is greater than one (signal greater than noise) for changes in soil moisture and severity in North Africa. The magnitude of these changes is therefore associated with high confidence especially under the 3 °C warming level. For the rest of projections, both over North Africa and Sahel, the SNR is less than one (dominance of noise), and thus are associated with substantial uncertainty. These results demonstrate that uncertainty in the ensemble median projections can largely differ between drought indicators (soil moisture versus runoff) and propagates nonlinearly into drought characteristics. The latter was also reported in Samaniego et al. (2017) and is attributed to the nonlinear behavior induced by the method used to identify drought events (drought only occurs if $SMI \leq 0.2$).

This substantial uncertainty highlights that using the “middle-of-the-road estimate” (ensemble median or mean) may provide misleading results because it does not consider the full range of possible futures. The uncertainty in the ensemble median is attributed to the high variability among ensemble members. Figure 3b presents the IMs and GCMs’ contribution to the total uncertainty. Overall, IMs show a comparable uncertainty contribution to GCMs for drought characteristics (GCM/IM ratio between 0.8 and 1.2) across North Africa and Sahel. GCMs, on the other hand, are considered the main contributor to uncertainty in changes in soil

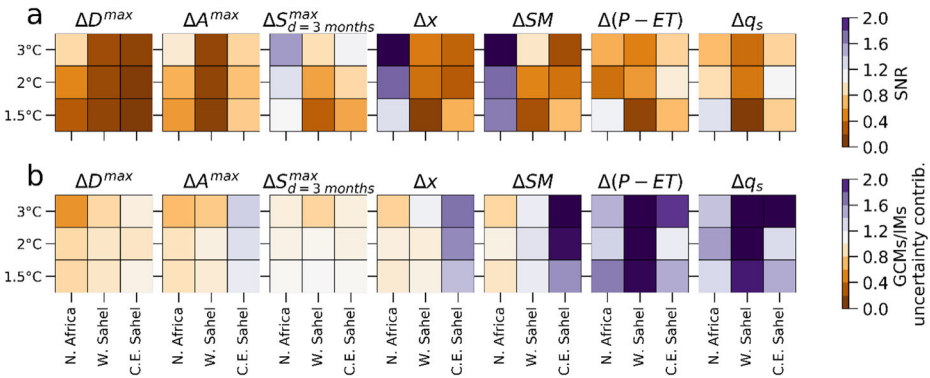


Fig. 3 Uncertainty assessment in drought projections. Upper row (a) presents the signal-to-noise ratio (SNR) calculated from changes (global warming levels minus historical period) in drought characteristics (presented in Fig. 1) of maximum drought events duration (ΔD^{max}), maximum drought area (ΔA^{max}), and maximum severity of 3-months droughts ($\Delta S^{max}_{d=3 \text{ months}}$), and drought indicators (presented in Fig. 2) of soil moisture under drought (Δx), mean soil moisture (ΔSM), mean precipitation minus evapotranspiration ($\Delta(P-ET)$), and mean surface runoff (Δq_s). SNR less than one indicates substantial uncertainty in model projections. Bottom row (b) presents the ratio between GCM and IM contributions to the total uncertainty. GCMs/IMs less than one indicates large IMs contribution to total uncertainty; values greater than one indicate high GCMs induced uncertainty

moisture over the central and eastern Sahel and hydrological drought indicators across the whole study domain (GCM/IM ratio greater than 1.2).

Differences in temporal soil moisture variability between IMs (particularly during dry months), which may not be substantial in a physical sense, when transformed into percentiles lead to substantial inter-model differences in terms of drought occurrence (Fig. S5). Such differences explain the substantial contribution of IMs to uncertainty in drought event characteristics. Inter-model differences originate from the substantially diverse representations of soil moisture, evapotranspiration, and runoff within IMs (Table S1). These different representations have greater effects as the hydrological cycle intensifies due to warmer conditions (Fig. S15). For instance, the method employed for evapotranspiration estimation is a key factor for drought analysis, especially in water-limited regimes where most moisture leaves the system through evaporation. Therefore, the representation of evapotranspiration, for example, in PCR-GLOBWB using temperature-based PET (i.e., the Hamon method) leads to a different evaporative response compared to solving the energy balance in LSMs (Fig. S16). Further works should therefore prioritize the characterization of uncertainty in GHMs/LSMs and reduce these uncertainties through improved process representation over semi-arid environments (Clark et al. 2016).

A dominant GCM contribution to uncertainty is expected since precipitation deficits are by definition the primary cause of droughts. The GCMs subset used in this study captures the inter-model variation in the amplitude of change in precipitation over the whole region (Fig. S14) and the opposite direction of trend across the Sahel. Nevertheless, we acknowledge that a higher GCM-induced uncertainty is expected from using a GCM sub-sample representative of the full CMIP5 ensemble spread (Monerie et al. 2017). To provide more comprehensive future drought trajectories, future works should also consider additional sources of uncertainty originating from the choice of bias-correction, downscaling procedure using regional climate experiments, choice of the baseline period, and internal climate variability.

4 Summary and conclusions

Global warming intensification results in a robust (>66% model agreement) exacerbation of soil moisture drought events duration, area, and severity across North Africa. Global warming between 1.5 and 3 °C leads to multi-year (from 12 to 19 years) mega-drought events. This unprecedented intensification implies that historical drought extremes could become normal conditions in the future (Lehner et al. 2017; Naumann et al. 2018; Samaniego et al. 2018). Similarly, historically severe 12-month drought events are projected to transform into exceptional events under 3 °C global warming. These events are expected to extend over an area that is 32% larger under the 3 °C warming level compared to the 1.5 °C level. Soil water availability under drought events is expected to decrease by up to 10% under a global warming of 3 °C. These changes are consistent with drying in hydrological drought indicators represented by P-ET and surface runoff and mainly result from an alteration of the hydrologic regime toward hyper-arid conditions due to a decline in rainfall as global warming intensifies.

Drought projections over the Sahel are mostly consistent (>66% model agreement) under the high global warming level of 3 °C. These projections suggest an intensification in exceptional drought event duration, especially over the western parts (of up to 82 months under 3 °C compared to 24 months under 1.5 °C), and increase in drought severity everywhere in the Sahel. This intensification of drought conditions is however in contrast to projections of a wetter central and eastern Sahel. Such a difference highlights that changes in the spatiotemporal characteristics of drought extremes can vary greatly from changes in mean drought indicators represented by precipitation, soil moisture, and runoff (Dai et al. 2018; Zhao and Dai 2015). Drought exacerbation in a wetter Sahel also indicates that rising atmospheric evaporative demand, mainly due to warming, will have a higher importance in driving drought intensification (Cook et al. 2018; Dai 2013).

The signal-to-noise ratio reveals large uncertainties associated with drought projections across the study area. This high degree of uncertainty indicates that using the “middle-of-the-road estimate” (ensemble median or mean) may provide misleading results because it does not consider the full range of possible futures. Uncertainties attributed to IMs are substantial, which further emphasizes the need to prioritize the characterization of uncertainty in GHMs/LSMs and reduce these uncertainties through improved process representation across semi-arid environments (Clark et al. 2016).

The findings of this study highlight the potential need to adapt to new normal conditions in the future. Unprecedented future droughts could pose serious threats to food security for a growing North African and Sahelian population. Further assessments are therefore needed to investigate the negative impacts of future drought extremes and evaluate possible mitigation strategies in the context of a multitude of uncertainties.

Supplementary Information The online version contains supplementary material available at <https://doi.org/10.1007/s10584-021-03202-0>.

Acknowledgements The authors are grateful to the Inter-Sectoral Impact Model Intercomparison Project modeling groups and the cross-sectoral science team for their roles in producing, coordinating, and making available the ISMIP models output. AE acknowledges support from Centre National pour la Recherche Scientifique et Technique (CNRST), Programme de Bourses d'Excellence de Recherche scholarship N°10UIZ2019. This study was carried out within the context of the CHARISMA project with the assistance of the Hassan 2 Academy of Sciences and Techniques and Ibn Zohr University. We would like to thank Sifeddine Afaf for proofreading the manuscript.

Author contribution AE, YP, ZEM, and LB conceived and designed the study. AE analyzed the data. All authors provided critical insights on the results and interpretation. AE drafted the manuscript, with a substantial contribution from YP, AC, AS, ST, and LB.

Data availability Monthly soil moisture projections are available via the ISIMIP ESGF server (<http://isimip.org/outputdata/isimip-data-on-the-esgf-server/>).

Code availability Code supporting the findings of this study is available from the Department of Computational Hydrosystems at the Helmholtz Centre for Environmental Research repository at <https://git.ufz.de/chs/progs/SMI>. Results data and code written to generate the figures are available from the corresponding author upon request.

Declarations Not applicable.

Consent to participate Not applicable.

Consent for publication Not applicable.

Competing interests The authors declare no competing interests.

References

- Andreadis KM, Clark EA, Wood AW, Hamlet AF, Lettenmaier DP (2005) Twentieth-century drought in the conterminous United States. *J Hydrometeorol* 6:985–1001. <https://doi.org/10.1175/JHM450.1>
- Bazza M, Melvyn K, Cody K (2018) Drought characteristics and management in North Africa and the Near East. Food and Agriculture Organization of the United Nations (FAO), National Drought Mitigation Center, University of Nebraska-Lincoln, USA
- Best MJ et al (2011) The Joint UK Land Environment Simulator (JULES), model description – part 1: energy and water fluxes. *Geosci Model Dev* 4:677–699. <https://doi.org/10.5194/gmd-4-677-2011>
- Biasutti M (2013) Forced Sahel rainfall trends in the CMIP5 archive. *J Geophys Res Atmos* 118:1613–1623. <https://doi.org/10.1002/jgrd.50206>
- Biasutti M, Sobel AH (2009) Delayed Sahel rainfall and global seasonal cycle in a warmer climate. *Geophys Res Lett* 36. <https://doi.org/10.1029/2009GL041303>
- Clark MP et al (2016) Characterizing uncertainty of the hydrologic impacts of climate change. *Curr Climate Change Rep* 2:55–64. <https://doi.org/10.1007/s40641-016-0034-x>
- Cook BI, Mankin JS, Anchukaitis KJ (2018) Climate change and drought: from past to future. *Curr Climate Change Rep* 4:164–179. <https://doi.org/10.1007/s40641-018-0093-2>
- Dai A (2013) Increasing drought under global warming in observations and models. *Nature Climate Change* 3: 52–58. <https://doi.org/10.1038/nclimate1633>
- Dai A, Zhao T, Chen J (2018) Climate change and drought: a precipitation and evaporation perspective. *Curr Climate Change Rep* 4:301–312. <https://doi.org/10.1007/s40641-018-0101-6>
- Diallo I, Sylla MB, Giorgi F, Gaye AT, Camara M (2012) Multimodel GCM-RCM ensemble-based projections of temperature and precipitation over West Africa for the early 21st century. *Intl J Geophys* 2012:972896. <https://doi.org/10.1155/2012/972896>
- Diedhiou A et al (2018) Changes in climate extremes over West and Central Africa at 1.5 °C and 2 °C global warming. *Environ Res Lett* 13:065020. <https://doi.org/10.1088/1748-9326/aac3e5>
- Dottori F et al (2018) Increased human and economic losses from river flooding with anthropogenic warming. *Nature Climate Change* 8:781–786. <https://doi.org/10.1038/s41558-018-0257-z>
- Droogers P, Immerzeel WW, Terink W, Hoogeveen J, Bierkens MFP, van Beek LPH, Debele B (2012) Water resources trends in Middle East and North Africa towards 2050. *Hydrol Earth Syst Sci* 16:3101–3114. <https://doi.org/10.5194/hess-16-3101-2012>
- Edward B et al (2018) Global exposure and vulnerability to multi-sector development and climate change hotspots. *Environ Res Lett* 13:055012
- Fontaine B, Roucou P, Monerie P-A (2011) Changes in the African monsoon region at medium-term time horizon using 12 AR4 coupled models under the A1b emissions scenario. *Atmospheric Science Letters* 12: 83–88. <https://doi.org/10.1002/asl.321>

- Frieler K et al (2017) Assessing the impacts of 1.5 °C global warming – simulation protocol of the Inter-Sectoral Impact Model Intercomparison Project (ISIMIP2b). *Geosci Model Dev* 10:4321–4345. <https://doi.org/10.5194/gmd-10-4321-2017>
- Godfray HCJ et al (2010) Food security: the challenge of feeding 9 billion people. *Science* 327:812. <https://doi.org/10.1126/science.1185383>
- Greve P, Orlowsky B, Mueller B, Sheffield J, Reichstein M, Seneviratne SI (2014) Global assessment of trends in wetting and drying over land. *Nature Geoscience* 7:716–721. <https://doi.org/10.1038/ngeo2247>
- Greve P, Seneviratne SI (2015) Assessment of future changes in water availability and aridity. *Geophys Res Lett* 42:5493–5499. <https://doi.org/10.1002/2015GL064127>
- Grillakis MG (2019) Increase in severe and extreme soil moisture droughts for Europe under climate change. *Sci Total Environ* 660:1245–1255. <https://doi.org/10.1016/j.scitotenv.2019.01.001>
- Grolle J (2015) Historical case studies of famines and migrations in the West African Sahel and their possible relevance now and in the future. *Popul Environ* 37:181–206
- Guimberteau M et al. (2018) ORCHIDEE-MICT (v8.4.1), a land surface model for the high latitudes: model description and validation *Geosci Model Dev* 11:121–163 <https://doi.org/10.5194/gmd-11-121-2018>
- Hanasaki N, Yoshikawa S, Pokhrel Y, Kanae S (2018) A global hydrological simulation to specify the sources of water used by humans. *Hydrol Earth Syst Sci* 22:789–817. <https://doi.org/10.5194/hess-22-789-2018>
- Hoegh-Guldberg O et al. (2018) Chapter 3: Impacts of 1.5°C global warming on natural and human systems. In: *Global warming of 1.5 °C an IPCC special report on the impacts of global warming of 1.5 °C above pre-industrial levels and related global greenhouse gas emission pathways, in the context of strengthening the global response to the threat of climate change*. Intergovernmental Panel on Climate Change (IPCC),
- Huang J, Ji M, Xie Y, Wang S, He Y, Ran J (2016) Global semi-arid climate change over last 60 years. *Climate Dynam* 46:1131–1150. <https://doi.org/10.1007/s00382-015-2636-8>
- IFAD (2010) Rural poverty report 2011. New realities, new challenges: new opportunities for tomorrow's generations. International Fund for Agricultural Development (IFAD), Rome, Italy
- IPCC (2012) Managing the risks of extreme events and disasters to advance climate change adaptation. . A Special Report of Working Groups I and II of the Intergovernmental Panel on Climate Change (IPCC). Cambridge University Press and New York, NY, USA,
- IPCC (2013) Climate change 2013: the physical science basis. Contribution of Working Group I to the Fifth Assessment Report of the Intergovernmental Panel on Climate Change. Cambridge University Press, Cambridge, United Kingdom and New York, NY, USA,
- James R, Washington R (2013) Changes in African temperature and precipitation associated with degrees of global warming *Climatic Change* 117:859–872 [doi:https://doi.org/10.1007/s10584-012-0581-7](https://doi.org/10.1007/s10584-012-0581-7)
- James R, Washington R, Jones R (2015) Process-based assessment of an ensemble of climate projections for West Africa. *J Geophys Res Atmos* 120:1221–1238. <https://doi.org/10.1002/2014JD022513>
- James R, Washington R, Schleussner C-F, Rogelj J, Conway D (2017) Characterizing half-a-degree difference: a review of methods for identifying regional climate responses to global warming targets. *Wiley Interdisc Rev Climate Change* 8:e457. <https://doi.org/10.1002/wcc.457>
- Kandji ST, Verchot L, Mackensen J (2006) Climate change and variability in the Sahel region: impacts and adaptation strategies in the agricultural sector. World Agroforestry Centre Nairobi, Kenya
- Keyantash J, Dracup JA (2002) The quantification of drought: an evaluation of drought indices *Bull Am Meteorol Soc* 83:1167–1180 [doi:https://doi.org/10.1175/1520-0477-83.8.1167](https://doi.org/10.1175/1520-0477-83.8.1167)
- Khan ZR, Midega CAO, Pitchar JO, Murage AW, Birkett MA, Bruce TJA, Pickett JA (2014) Achieving food security for one million sub-Saharan African poor through push-pull innovation by 2020. *Philos Trans Royal Soc B Biol Sci* 369:20120284. <https://doi.org/10.1098/rstb.2012.0284>
- Klutse NAB et al (2018) Potential impact of 1.5 °C and 2 °C global warming on consecutive dry and wet days over West Africa. *Environ Res Lett* 13:055013. <https://doi.org/10.1088/1748-9326/aab37b>
- Konapala G, Mishra A (2017) Review of complex networks application in hydroclimatic extremes with an implementation to characterize spatio-temporal drought propagation in continental USA. *J Hydrol* 555:600–620. <https://doi.org/10.1016/j.jhydrol.2017.10.033>
- Koster RD, Guo Z, Yang R, Dirmeyer PA, Mitchell K, Puma MJ (2009) On the nature of soil moisture in land surface models. *J Climate* 22:4322–4335. <https://doi.org/10.1175/2009JCLI2832.1>
- Lange S et al. (2020) Projecting exposure to extreme climate impact events across six event categories and three spatial scales *Earth's Future* 8:e2020EF001616 [doi:https://doi.org/10.1029/2020EF001616](https://doi.org/10.1029/2020EF001616)
- Lehner F, Coats S, Stocker TF, Pendergrass AG, Sanderson BM, Raible CC, Smerdon JE (2017) Projected drought risk in 1.5°C and 2°C warmer climates. *Geophys Res Lett* 44:7419–7428. <https://doi.org/10.1002/2017GL074117>
- Mach KJ et al. (2019) Climate as a risk factor for armed conflict *Nature* 571:193–197 [doi:10.1038/s41586-019-1300-6](https://doi.org/10.1038/s41586-019-1300-6)
- Maharatna A (2014) Food scarcity and migration: an overview social research 81:277–298

- Mariotti L, Coppola E, Sylla MB, Giorgi F, Piani C (2011) Regional climate model simulation of projected 21st century climate change over an all-Africa domain: comparison analysis of nested and driving model results *Journal of Geophysical Research: Atmospheres* 116 doi:<https://doi.org/10.1029/2010JD015068>
- Masih I, Maskey S, Mussá FEF, Trambauer P (2014) A review of droughts on the African continent: a geospatial and long-term perspective. *Hydrol Earth Syst Sci* 18:3635–3649. <https://doi.org/10.5194/hess-18-3635-2014>
- Mishra AK, Singh VP (2010) A review of drought concepts. *J Hydrol* 391:202–216. <https://doi.org/10.1016/j.jhydrol.2010.07.012>
- Monerie P-A, Sanchez-Gomez E, Boé J (2017) On the range of future Sahel precipitation projections and the selection of a sub-sample of CMIP5 models for impact studies. *Climate Dynamics* 48:2751–2770. <https://doi.org/10.1007/s00382-016-3236-y>
- Müller Schmied H et al (2016) Variations of global and continental water balance components as impacted by climate forcing uncertainty and human water use. *Hydrol Earth Syst Sci* 20:2877–2898. <https://doi.org/10.5194/hess-20-2877-2016>
- Naumann G et al (2018) Global changes in drought conditions under different levels of warming. *Geophys Res Lett* 45:3285–3296. <https://doi.org/10.1002/2017GL076521>
- Niang et al. (2014a) Chapter 22 Africa. In: *Climate Change 2014: Impacts, adaptation, and vulnerability. Part B: regional aspects. Contribution of Working Group II to the Fifth Assessment Report of the Intergovernmental Panel on Climate Change* In pp 1199–1265
- Niang I, O.C. Ruppel, M.A. Abdrabo, A. Essel, C. Lennard, J. Padgham, and P. Urquhart (2014b) Africa. In: *Intergovernmental Panel on Climate C (ed) Climate Change 2014 – impacts, adaptation and vulnerability: part B: regional aspects: Working Group II Contribution to the IPCC Fifth Assessment Report: Volume 2: Regional Aspects, vol 2. Cambridge University Press, Cambridge, pp 1199–1266. doi:DOI: https://doi.org/10.1017/CBO9781107415386.002*
- Orlowsky B, Seneviratne SI (2013) Elusive drought: uncertainty in observed trends and short- and long-term CMIP5 projections. *Hydrol Earth Syst Sci* 17:1765–1781. <https://doi.org/10.5194/hess-17-1765-2013>
- Park J-Y, Bader J, Matei D (2015) Northern-hemispheric differential warming is the key to understanding the discrepancies in the projected Sahel rainfall. *Nature Commun* 6:5985. <https://doi.org/10.1038/ncomms6985>
- Pokhrel Y et al (2021) Global terrestrial water storage and drought severity under climate change. *Nature Climate Change*. <https://doi.org/10.1038/s41558-020-00972-w>
- Pokhrel Y et al (2012) Incorporating anthropogenic water regulation modules into a land surface model. *J Hydrometeorol* 13:255–269. <https://doi.org/10.1175/JHM-D-11-013.1>
- Pokhrel YN, Koirala S, Yeh PJF, Hanasaki N, Longuevergne L, Kanae S, Oki T (2015) Incorporation of groundwater pumping in a global Land Surface Model with the representation of human impacts. *Water Resour Res* 51:78–96. <https://doi.org/10.1002/2014WR015602>
- Polade SD, Gershunov A, Cayan DR, Dettinger MD, Pierce DW (2017) Precipitation in a warming world: assessing projected hydro-climate changes in California and other Mediterranean climate regions. *Sci Rep* 7: 10783. <https://doi.org/10.1038/s41598-017-11285-y>
- Prudhomme C et al (2014) Hydrological droughts in the 21st century, hotspots and uncertainties from a global multimodel ensemble experiment. *Proc Natl Acad Sci* 111:3262. <https://doi.org/10.1073/pnas.1222473110>
- Roudier P, Sultan B, Quirion P, Berg A (2011) The impact of future climate change on West African crop yields: what does the recent literature say? *Glob Environ Chang* 21:1073–1083. <https://doi.org/10.1016/j.gloenvcha.2011.04.007>
- Samaniego L et al (2017) Propagation of forcing and model uncertainties on to hydrological drought characteristics in a multi-model century-long experiment in large river basins. *Climatic Change* 141:435–449. <https://doi.org/10.1007/s10584-016-1778-y>
- Samaniego L, Kumar R, Zink M (2013) Implications of parameter uncertainty on soil moisture drought analysis in Germany. *J Hydrometeorol* 14:47–68. <https://doi.org/10.1175/JHM-D-12-075.1>
- Samaniego L et al (2018) Anthropogenic warming exacerbates European soil moisture droughts. *Nature Climate Change* 8:421–426. <https://doi.org/10.1038/s41558-018-0138-5>
- Samaniego L et al (2019) Hydrological forecasts and projections for improved decision-making in the water sector in Europe. *Bull Am Meteorol Soc* 100:2451–2472. <https://doi.org/10.1175/BAMS-D-17-0274.1>
- Scheff J, Frierson DMW (2014) Scaling potential evapotranspiration with greenhouse warming. *J Climate* 27: 1539–1558. <https://doi.org/10.1175/JCLI-D-13-00233.1>
- Schewe J et al. (2019) State-of-the-art global models underestimate impacts from climate extremes *Nature Commun* 10:1005 doi:<https://doi.org/10.1038/s41467-019-08745-6>
- Schilling J, Freier KP, Hertig E, Scheffran J (2012) Climate change, vulnerability and adaptation in North Africa with focus on Morocco agriculture. *Ecosystems & Environment* 156:12–26. <https://doi.org/10.1016/j.agee.2012.04.021>
- Schilling J, Hertig E, Trambly Y, Scheffran J (2020) Climate change vulnerability, water resources and social implications in North Africa. *Region Environ Chang* 20:15. <https://doi.org/10.1007/s10113-020-01597-7>

- Seth A, Rauscher SA, Biasutti M, Giannini A, Camargo SJ, Rojas M (2013) CMIP5 projected changes in the annual cycle of precipitation in monsoon regions. *J Climate* 26:7328–7351. <https://doi.org/10.1175/JCLI-D-12-00726.1>
- Sheffield J, Andreadis KM, Wood EF, Lettenmaier DP (2009) Global and continental drought in the second half of the twentieth century: severity–area–duration analysis and temporal variability of large-scale events. *J Climate* 22:1962–1981
- Sheffield J, Wood EF (2008) Projected changes in drought occurrence under future global warming from multi-model, multi-scenario, IPCC AR4 simulations. *Climate Dynam* 31:79–105. <https://doi.org/10.1007/s00382-007-0340-z>
- Sitch S et al (2003) Evaluation of ecosystem dynamics, plant geography and terrestrial carbon cycling in the LPJ dynamic global vegetation model. *Global Change Biol* 9:161–185. <https://doi.org/10.1046/j.1365-2486.2003.00569.x>
- Sultan B, Gaetani M (2016) Agriculture in West Africa in the twenty-first century: climate change and impacts scenarios, and potential for adaptation. *Front Plant Sci* 7:1262
- Svoboda M et al (2002) The drought monitor. *Bull Am Meteorol Soc* 83:1181–1190
- Sylla MB, Giorgi F, Pal JS, Gibba P, Kebe I, Nikiema M (2015) Projected changes in the annual cycle of high-intensity precipitation events over West Africa for the late twenty-first century. *J Climate* 28:6475–6488. <https://doi.org/10.1175/JCLI-D-14-00854.1>
- Takata K, Emori S, Watanabe T (2003) Development of the minimal advanced treatments of surface interaction and runoff. *Global Planet Change* 38:209–222. [https://doi.org/10.1016/S0921-8181\(03\)00030-4](https://doi.org/10.1016/S0921-8181(03)00030-4)
- Thiery W, Davin EL, Lawrence DM, Hirsch AL, Hauser M, Seneviratne SI (2017) Present-day irrigation mitigates heat extremes. *J Geophys Res Atmos* 122:1403–1422. <https://doi.org/10.1002/2016JD025740>
- Tramblay Y et al (2020) Challenges for drought assessment in the Mediterranean region under future climate scenarios. *Earth-Sci Rev* 210:103348. <https://doi.org/10.1016/j.earscirev.2020.103348>
- Veldkamp TIE et al (2018) Human impact parameterizations in global hydrological models improve estimates of monthly discharges and hydrological extremes: a multi-model validation study. *Environ Res Lett* 13:055008. <https://doi.org/10.1088/1748-9326/aab96f>
- Vergopolan N et al (2021) Field-scale soil moisture bridges the spatial-scale gap between drought monitoring and agricultural yields. *Hydrol Earth Syst Sci* 25:1827–1847. <https://doi.org/10.5194/hess-25-1827-2021>
- Vgen T-G, Gumbrecht T (2012) Sahel atlas of changing landscapes: tracing trends and variations in vegetation cover and soil condition. UNEP
- von Uexkull N, Croicu M, Fjelde H, Buhaug H (2016) Civil conflict sensitivity to growing-season drought. *Proc Natl Acad Sci* 113:12391. <https://doi.org/10.1073/pnas.1607542113>
- Wada Y, Wisser D, Bierkens MFP (2014) Global modeling of withdrawal, allocation and consumptive use of surface water and groundwater resources. *Earth Syst Dynam* 5:15–40. <https://doi.org/10.5194/esd-5-15-2014>
- Wanders N, Van Loon AF, Van Lanen HAJ (2017) Frequently used drought indices reflect different drought conditions on global scale. *Hydrol Earth Syst Sci Discuss* 2017:1–16. <https://doi.org/10.5194/hess-2017-512>
- Wang A, Lettenmaier DP, Sheffield J (2011) Soil moisture drought in China, 1950–2006. *J Clim* 24:3257–3271. <https://doi.org/10.1175/2011JCLI3733.1>
- Wang G (2005) Agricultural drought in a future climate: results from 15 global climate models participating in the IPCC 4th assessment. *Climate Dynam* 25:739–753. <https://doi.org/10.1007/s00382-005-0057-9>
- Wartenburger R, Hirschi M, Donat MG, Greve P, Pitman AJ, Seneviratne SI (2017) Changes in regional climate extremes as a function of global mean temperature: an interactive plotting framework. *Geosci Model Dev* 10:3609–3634. <https://doi.org/10.5194/gmd-10-3609-2017>
- WMO (2018) Guidelines on the definition and monitoring of extreme weather and climate events. World Meteorological Organization Commission for Climatology, World Meteorological Organization Commission for Climatology
- Xu C et al (2019) Increasing impacts of extreme droughts on vegetation productivity under climate change. *Nature Climate Change* 9:948–953. <https://doi.org/10.1038/s41558-019-0630-6>
- Zaherpour J et al (2018) Worldwide evaluation of mean and extreme runoff from six global-scale hydrological models that account for human impacts. *Environ Res Lett* 13:065015
- Zhan W, He X, Sheffield J, Wood EF (2020) Projected seasonal changes in large-scale global precipitation and temperature extremes based on the CMIP5 ensemble. *J Climate* 33:5651–5671. <https://doi.org/10.1175/JCLI-D-19-0311.1>
- Zhao T, Dai A (2015) The magnitude and causes of global drought changes in the twenty-first century under a low–moderate emissions scenario. *J Climate* 28:4490–4512. <https://doi.org/10.1175/JCLI-D-14-00363>

Affiliations

Ahmed Elkouk^{1,2,3} · **Zine El Abidine El Morjani**¹ · **Yadu Pokhrel**³ ·
Abdelghani Chehbouni^{4,5} · **Abdelfattah Sifeddine**⁶ · **Stephan Thober**⁷ ·
Lhoussaine Bouchaou^{2,5}

¹ Ibn Zohr University, Faculty Polydisciplinary, Taroudant, Morocco

² Laboratory of Applied Geology and Geo-Environment, Faculty of Science, Ibn Zohr University, 80035 Agadir, Morocco

³ Department of Civil and Environmental Engineering, Michigan State University, East Lansing, MI 48824, USA

⁴ Centre d'Etudes Spatiales de la Biosphère (CESBIO), Université de Toulouse, CNRS, CNES, IRD, BPI 280, Toulouse Cedex 9, France

⁵ International Water Research Institute, Mohammed VI Polytechnic University, 43150 Ben Guerir, Morocco

⁶ IRD-Sorbonne Université, UMR LOCEAN (IRD, CNRS, Univ. Sorbonne, MNHN), Paris, France

⁷ Department of Computational Hydrosystems, Helmholtz Centre for Environmental Research – UFZ, Leipzig, Germany